8.18

AIRBORNE COHERENT LIDAR FOR ADVANCED IN-FLIGHT MEASUREMENTS (ACLAIM) FLIGHT TESTING OF THE LIDAR SENSOR

David C. Soreide*
Boeing Defense and Space Group
Seattle, Washington

Rodney K. Bogue and L. J. Ehernberger
NASA Dryden Flight Research Center
Edwards, California

Stephen M. Hannon
Coherent Technologies Inc.
Lafayette, Colorado

David A. Bowdle
University of Alabama
Huntsville, Alabama

1. PURPOSE

The purpose of the ACLAIM program is ultimately to establish the viability of light detection and ranging (lidar) as a forward-looking sensor for turbulence. The goals of this flight test are to: 1) demonstrate that the ACLAIM lidar system operates reliably in a flight test environment, 2) measure the performance of the lidar as a function of the aerosol backscatter coefficient (β), 3) use the lidar system to measure atmospheric turbulence and compare these measurements to onboard gust measurements, and 4) make measurements of the aerosol backscatter coefficient, its probability distribution and spatial distribution. The scope of this paper is to briefly describe the ACLAIM system and present examples of ACLAIM operation in flight, including comparisons with independent measurements of wind gusts, gust-induced normal acceleration, and the derived eddy dissipation rate.

2. EXPERIMENT DESCRIPTION

The aircraft platform used for this test, and the workings of the lidar system are described in this section. Field operations relating to these tests are also discussed.

2.1 Aircraft

The aircraft platform for the ACLAIM test flights was a Lockheed L-188C Electra (photo, fig. 2.1-1), which is operated by the National Center of Atmospheric Research (NCAR) in Boulder, Colorado, on behalf of the National Science Foundation.

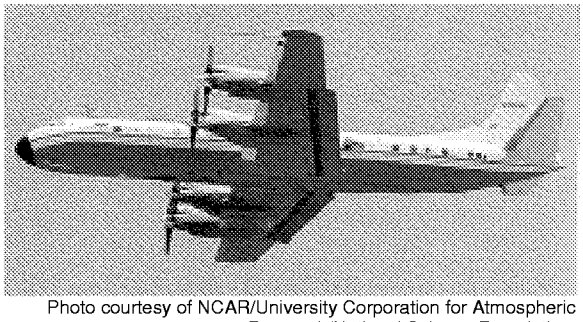

Photo courtesy of NCAR/University Corporation for Atmospheric Research/National Science Foundation.

Figure 2.1-1 Electra L-188C aircraft.

The Electra is a four-engine turboprop, with a maximum airspeed of 310 kn (160 m/s) and an operating ceiling of 28,000 ft (8.4 km). Various universities and national or international agencies routinely use this aircraft for a wide variety of basic and applied atmospheric research. The relatively low airspeed of the Electra is well suited for detailed studies of episodic turbulence and for small-scale atmospheric aerosol concentration features that may affect ACLAIM performance.

2.2 ACLAIM Lidar

The underlying principle of pulsed lidar measurement of wind and aerosols is the use of optical heterodyne (coherent) detection, in which laser pulses are transmitted into the atmosphere and scattered off of naturally-occurring small dust particles (aerosols) entrained in the ambient flow field. (Frehlich, Hannon, and Henderson (1998); Frehlich, Hannon, and

* David C. Soreide, Boeing Defense and Space Group, P.O.Box 3999, m/s 8H-18, Seattle, WA 98124; e-mail david.c.soreide@boeing.com

Henderson (1994); Huffaker and Hardesty (1996); and Soreide, et al. (1997)). The transmitted pulse is frequency offset from both the master oscillator and local oscillator (LO) by an intermediate frequency (μ_{i-f}) using an acoustooptic modulator (AOM) between the master oscillator laser and the pulsed slave laser. Because the value of μ_{i-f} can vary randomly from pulse to pulse (frequency jitter of a few MHz or less), a small fraction of the transmitted pulse is split off for the purpose of generating a pulse monitor signal at the output of a secondary photodetector. The backscattered laser energy is Doppler-shifted in frequency by an amount $\Delta\mu$ proportional to the velocity of the aerosols that are parallel to the direction of propagation of the illuminating laser (the radial velocity). The returned backscatter light is collected by the telescope and is combined with light from the LO on the surface of a photodetector. The light from the pulse sample is combined with light from the LO on the surface of a second photodetector to provide a pulse monitor signal useful for frequency offset and temporal jitter correction in the signal processor. The resultant i-f photocurrent contains a heterodyne term consisting of the difference frequency between the backscattered light (or pulse monitor light in the case of the monitor photodetector) and the LO. For the ACLAIM lidar system, the LO-induced shot noise dominates all other noise sources (for example, detector dark current and amplifier or thermal noise) and quantum-limited detection is achieved. That LO shot noise is typically 10 dB larger than all other noise sources combined over the entire i-f passband. The Doppler frequency shift is $\Delta\mu = 2v_r/\lambda$, where v_r is the radial velocity and λ is the operating wavelength. For 2-μm coherent lidar systems, the frequency shift is roughly 1 MHz/m/sec of particle velocity. The measurement range capability for the ACLAIM sensor is dependent on the distribution of naturally occurring atmospheric aerosols. In general, the aerosol density is larger near the surface of the earth, within the planetary boundary layer (PBL). Within the mid-troposphere above the PBL, the backscatter level drops to a lower level, a factor of 10 to 100 below the PBL. The lowest aerosol concentrations and levels of 2-μm backscatter are generally present in the upper troposphere, in the altitude range of 8–11 km. Above the tropopause, the backscatter level often increases slightly, due to the influence of high altitude photochemical aerosol production and residual volcanic ash.

The three figures in this section demonstrate the system just described. Nominal 2-μm aerosol backscatter values are illustrated in Figure 2.2-1 relative to 3×10^{-10} per m-sr (meter-steradian). Figure 2.2-2 shows aerosol backscatter distribution and figure 2.2-3 is a block diagram of the lidar.

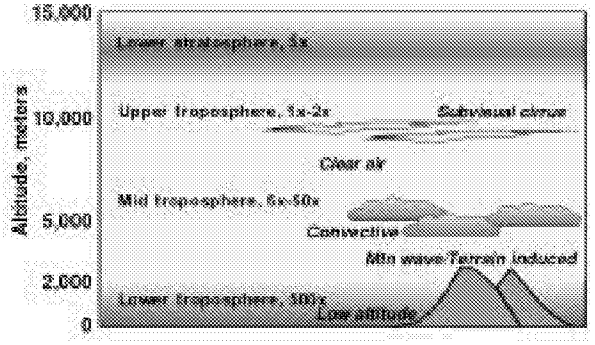

Figure 2.2-2 General distribution of atmospheric aerosol backscatter for the ACLAIM pulsed Doppler lidar.

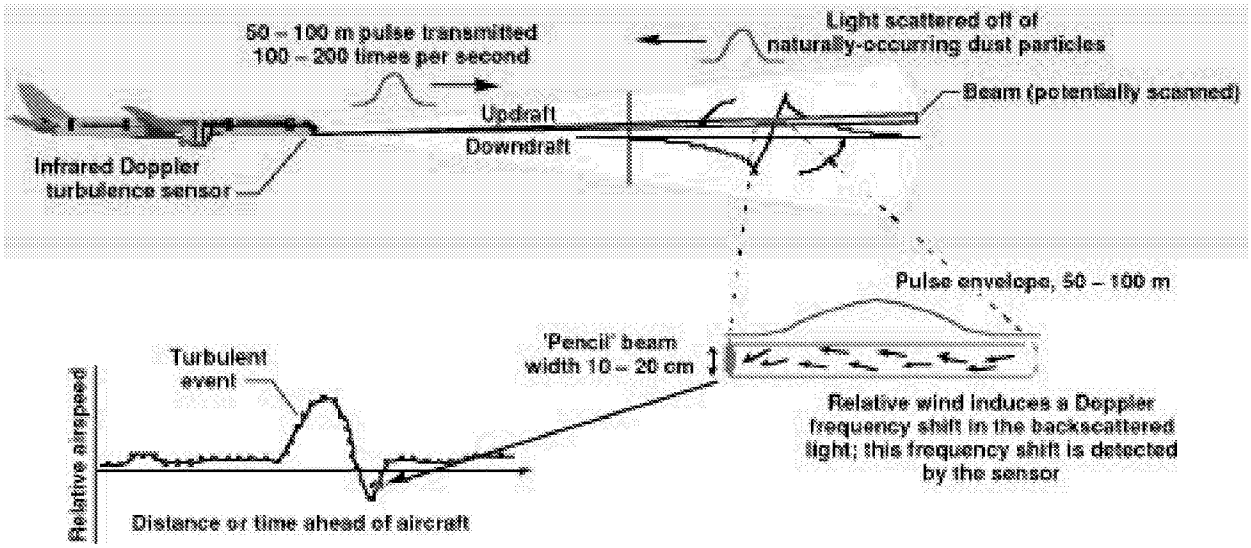

Figure 2.2-1 Pulsed Doppler lidar general principle of operation for airborne turbulence detection.

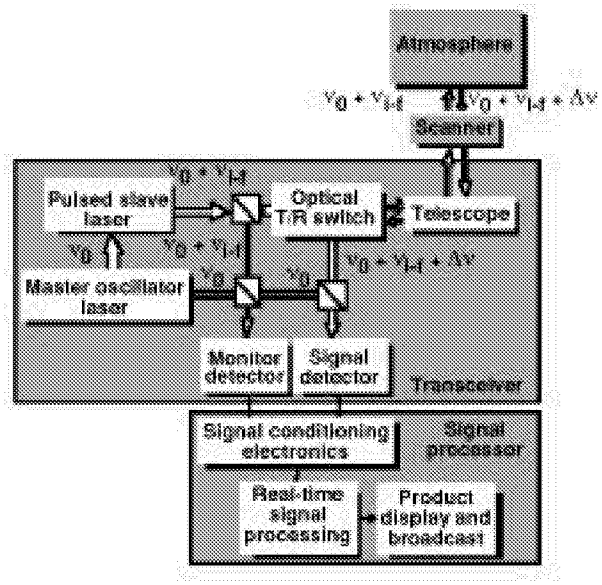

Figure 2.2-3 Block diagram of the ACLAIM lidar system.

The major subsystems are the transceiver and the signal processor. Not shown in the block diagram is the system controller and graphical user interface. This is the subsystem used by the system operator for monitor and control purposes. At the time of the Electra flight tests, the ACLAIM system did not have a scanner, so that only single line-of-sight measurements were made during the measurements. A scanner has been recently designed and constructed for integration with ACLAIM.

2.3 Field Operations

For the Spring 1998 test flights, the standard ACLAIM transmitter was replaced by a similar laser transmitter that Coherent Technologies, Inc. (Lafayette, Colorado) developed for the U.S. Air Force Wright Laboratories. The substitute transmitter provided an optical output of 1.2 watts (12 milliJoules @ 100 Hz). The modified ACLAIM system was mounted in the forward cabin of the Electra. A beam expander directed the output beam to a folding mirror housing on the outside of a modified aircraft window frame. The folding mirror directed the beam through a forward-viewing optical window, along a line of sight approximately 2 deg below and 0.5 deg to the left of the aircraft longitudinal axis. This fixed rigging angle compensated for a typical pitch angle of +2 deg in level flight on the Electra, so that the lidar beam normally pointed along the flight path. The mirror housing and the exit window were pressure sealed against the air outside the aircraft. The housing was continually purged with dry air to prevent condensation on the mirror and the inside surface of the exit window.

During the spring 1998 tests, ground-based calibrations against a diffuse planar hard target were conducted before and after every flight. For these calibrations, the lidar was usually focused at ~400 m, just beyond the minimum range, and the target (flame-sprayed aluminum) was placed at the focal plane. In addition, some calibration runs used the unexpanded collimated beam at the same range. For the first few calibrations, the Electra nose pointed toward the calibration target, with the nose wheel jacked up to lift the beam off the ground. For later calibrations, the Electra nose pointed perpendicular to the target line of sight, while a secondary external folding mirror directed the beam to the target. These calibrations provided a baseline for detecting and diagnosing any drift or abrupt changes in the lidar optical efficiency that may have developed in flight or between flights. They also provided an absolute radiometric calibration reference for the aerosol backscatter measurements.

3. FLIGHT TEST RESULTS

Transmitter performance and stability as well as velocity and turbulence measurements are discussed in this section. Elaborations of axial velocity gust comparisons and turbulent product measurements are shown also.

3.1 Transmitter Performance/Stability

The laser power, after the system was installed on the airplane, was 12 milliJoules. This power was held constant over the test period. The pulse repetition frequency of 100 Hz varied by less than 1 percent over the course of the flight test. Vibration levels were lower than levels used in the acceptance testing and no degradation of the lidar performance resulting from vibration was observed.

System stability is also related to the fraction of transmit-pulses that were well-seeded (single frequency locked to the seed laser). The fraction of seeded pulses is estimated to be well in excess of 99 percent, indicating very stable operation for the sensor.

3.2 Velocity and Turbulence Measurements

In this report data are reported from several turbulence encounters generated by the Wet Mountains near Pueblo, Colorado. These data were chosen because they represent the largest turbulence intensity encountered on the flights, have a clear transition from smooth to turbulent air, and are characteristic of a class of turbulence which is commonly encountered by commercial flights. Figure 3.2-1 is an overview plot of the vertical velocity from the aircraft gust probe (labeled XWIC) as a function of time on a typical flight track, flying upwind through the mountain wave.

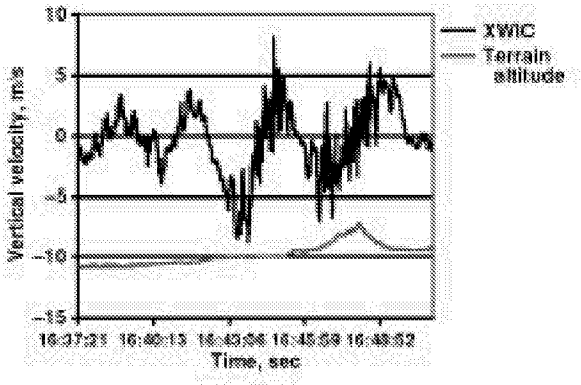

Figure 3.2-1 Overview of mountain wave flow field.

Turbulence was not encountered throughout the mountain wave, but only in the downslope wind in the first two waves downstream of the ridge.

The terrain altitude is co-plotted only to indicate where the mountain wave is with respect to the terrain. The height at the ridge peak is 1700 m above the level at the beginning of the flight leg. As noted above, the velocity data were acquired using the airplane gust probe system.

3.2.1 Axial Velocity Gust Comparisons

Using the lidar to predict the existence of disturbances is one of the main goals of this program, and this capability was clearly demonstrated. A number of gusts were identified on the real time display, tracked as they approached the aircraft, and felt, as the airplane penetrated the disturbed region. Figures 3.2.1-1a through 3.2.1-1e are a set of snapshots from the real time display as the airplane encountered what was the largest gust of the flight test program.

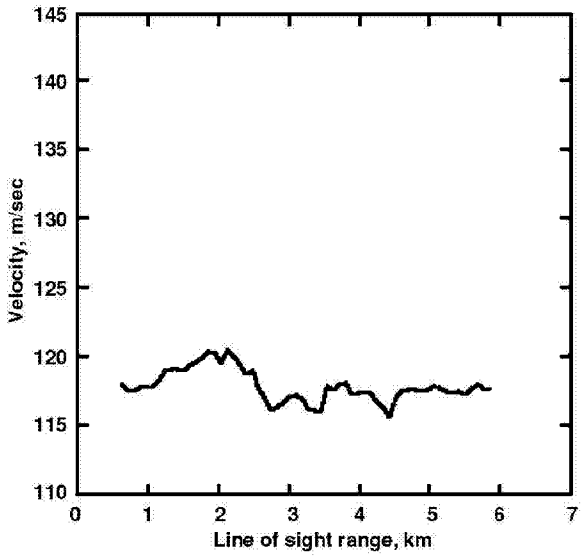

Figure 3.2.1-1a ACLAIM Display (t = 0 sec).

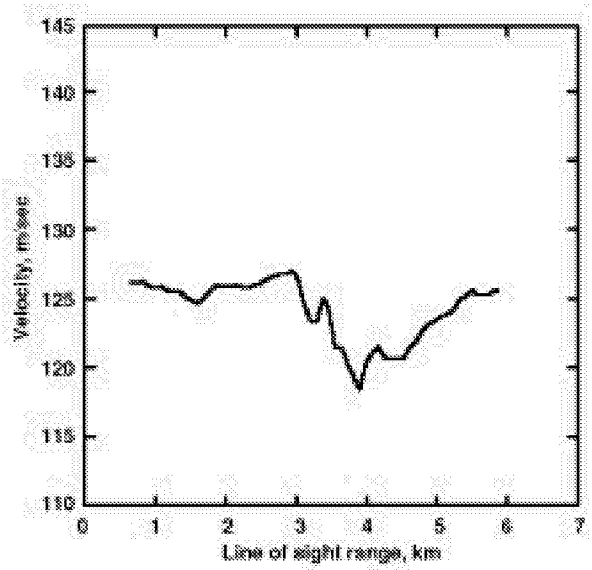

Figure 3.2.1-1b ACLAIM Display (t = 34 sec).

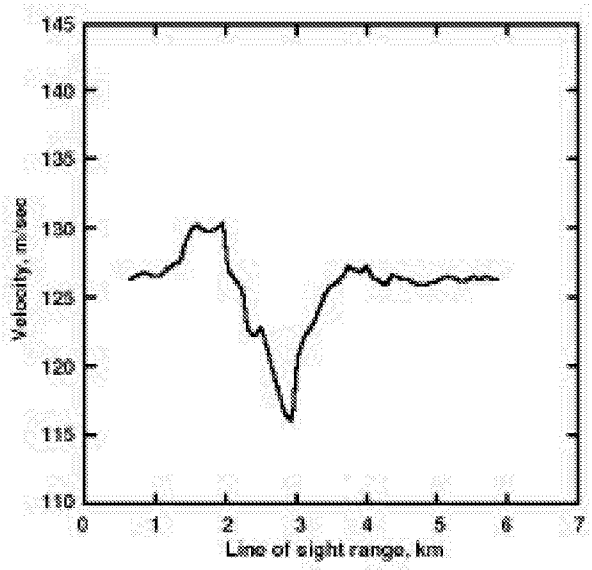

Figure 3.2.1-1c ACLAIM Display (t = 42 sec).

At time = 0 the air ahead of the airplane was quiescent, with no disturbance. At time = 34 sec we can see a disturbance at 4 km. In the next two frames t = 42 and 46 sec the disturbance can be tracked, approaching the airplane. At t = 62 (time = 17:16:10-15) there were a series of vertical accelerations, the largest of which had a peak to peak value of ~.45 g. If we compare the axial velocity measured with the lidar to the axial velocity measured with the airplane gust probe, we can evaluate quantitatively how well the system predicts velocity disturbances. The data shown in figure 3.2.1-2 are a comparison of the lidar data taken at a range of 1088 m with data taken at the gust probe. As the flight test airplane traversed the large-scale mountain waves, the

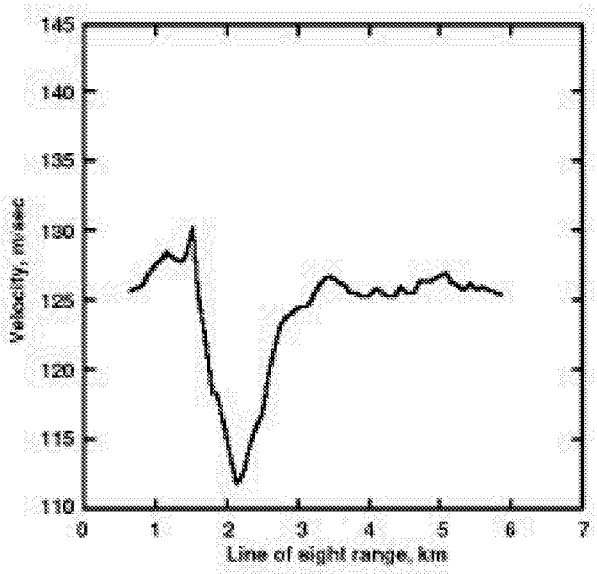

Figure 3.2.1-1d ACLAIM Display (t = 46 sec).

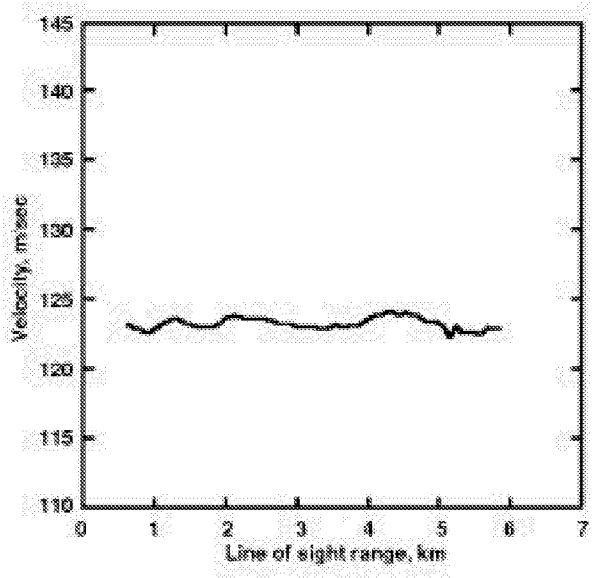

Figure 3.2.1-1e ACLAIM Display (t = 62 sec).

airspeed varied by ±10 m/s or more. This gross motion obscures the smaller fluctuations in wind speed, those gusts that we measure with the lidar. In order to reduce the gross airplane variations in airspeed, the airplane velocity at the time of the lidar measurement was subtracted from both the lidar and airplane gust probe time series.

For comparison between the lidar measurements and the subsequent measurements at the time of aircraft encounter, lidar data were selected for a distance of 1088 m ahead of the airplane. Atmospheric wind and gust changes during the travel time over this distance are

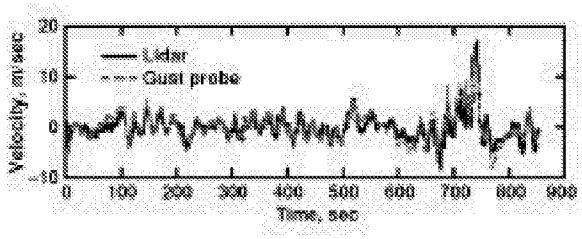

Figure 3.2.1-2 Comparison of lidar and airplane gust probe data.

minimal and lidar wild points at this range were essentially nonexistent. In this plot the lidar data is lagged by 9 sec so that we can compare it with the airplane measurement of the same air mass. For fluctuations in the .1-Hz range, the agreement is remarkably good. For somewhat higher frequencies, there is increased data scatter. In order to quantify the agreement between these data, we calculate the correlation coefficient between the lidar and gust probe data. The cross-correlation function is shown in figure 3.2.1-3.

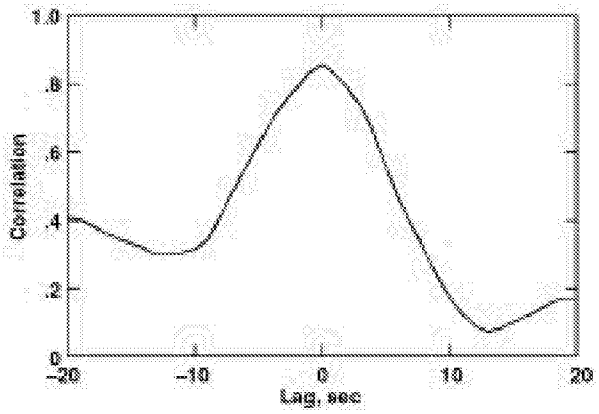

Figure 3.2.1-3 Cross-correlation coefficient between lidar and gust probe velocity.

The maximum correlation coefficient of .86 indicates good agreement between the two data sets over a 15-min flight segment that includes the flight leg shown in figure 3.2.1-2.

The selection of a turbulence product is outside the scope of this document, but some presentation of proposed turbulence products is necessary to demonstrate the performance of the system. There are several possibilities, all of which devolve to a measurement of the velocity fluctuations in a "sensible" bandwidth. The simplest parameter is the standard deviation of the lidar signal. We have calculated the standard deviation of overlapping sets of 5 data points. In figure 3.2.2-1 this is compared with the normal acceleration.

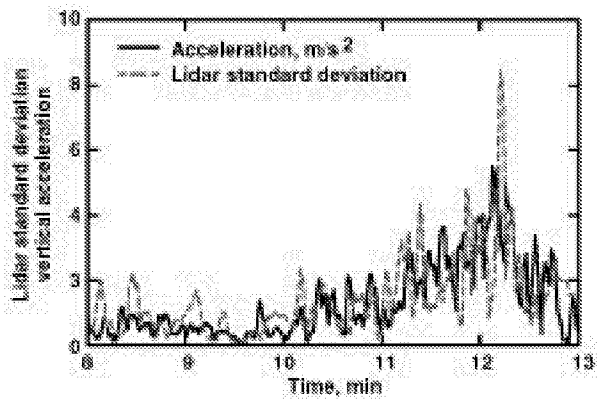

Figure 3.2.2-1 Comparison of the normal acceleration with the standard deviation of the lidar signal.

To allow for the advance lidar detection range used in this example a 6-sec lag was applied to illustrate the correspondence between the lidar prediction and the airplane response. We must point out that this is not the maximum possible warning, but a convenient value for the analysis. Data was available to warning times of as much as 100 sec and provided successful detections at ranges of 5–8 km with postflight outlier-removal procedures. The turbulent encounter shown in this plot is from flight number 2, and shows strong turbulence. We can see by inspection that the increase in vertical acceleration is predicted quite well.

A second parameter that presents the variation in the velocity in a band-limited fashion is the structure function. Figure 3.2.2-2 is a plot of the structure function of the axial velocity measured by the lidar with a separation distance of 797 m [1333 m ahead of the airplane (~11-sec warning)]. The disturbance at one minute is clearly predicted by the lidar.

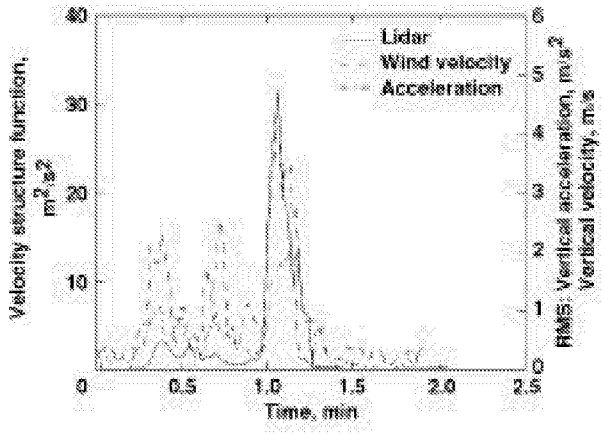

Figure 3.2.2-2 Velocity structure function for a turbulent event in flight 2.

A third parameter representing the velocity disturbance in a frequency band is the eddy dissipation rate, epsilon (ε). This parameter is more complex to calculate than the previous two, but is preferred, because of its use both in atmospheric science and previous modeling of the supersonic inlet unstart rate (Soreide, Bogue, and Seidel (1997)).

The eddy dissipation rate is calculated from the structure function using

$$S(x) = 2\varepsilon^{\frac{2}{3}} x^{\frac{2}{3}} \qquad (1)$$

Where $S(x)$ is the structure function, which is a function of x (the separation) and ε (the eddy dissipation rate).

As a first step, let us compare the eddy dissipation rate to the vertical acceleration, using the airplane instrumentation. This comparison gives us some confidence that the eddy dissipation rate is indeed a viable measure of turbulence and a reasonable predictor of increased variation in the vertical acceleration. The eddy dissipation rate, ε, is calculated by computing the structure function $S(x)$ over a 5-sec (~600 m) time window at three separations (120 m, 240 m and 360 m) and using a least-squares fit to compute ε.

In order to estimate the predictive power of the eddy dissipation rate, we take the standard deviation of accelerations measured at a given value of ε. From these data, we can construct figure 3.2.2-3.

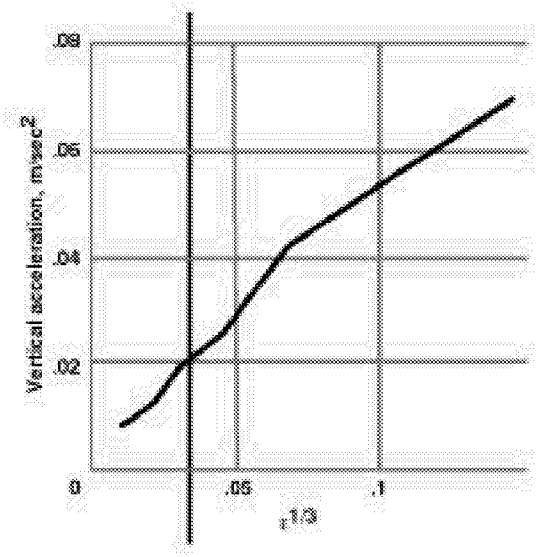

Figure 3.2.2-3 Variation in the vertical acceleration and the cube root of eddy dissipation rate.

This plot clearly indicates that increased vertical accelerations are statistically predicted by elevated values of ε. That is, the eddy dissipation rate is closely correlated to the variation in the vertical acceleration. Here we have plotted the 1/3 power of epsilon, which is linearly related to the standard deviation, and can be shown to be linearly related to the vertical acceleration of the airplane (Bowles, (1998)). The cross-correlation between epsilon and vertical acceleration is .87 for the data in figure 3.2.2-3. If we then use the lidar to predict the eddy dissipation rate, we are faced with a somewhat more complex calculation. The data presented in this section uses the approach outlined above, and is repeated during the time that a given air packet is visible using the lidar data. We must point out that cross-correlations emphasize the larger ε values. So this is not a measure of the uncertainty of ε at the airplane given the lidar-derived ε. A comparison of the airplane-derived measure of ε and the lidar-derived measure of ε is shown in figure 3.2.2-4.

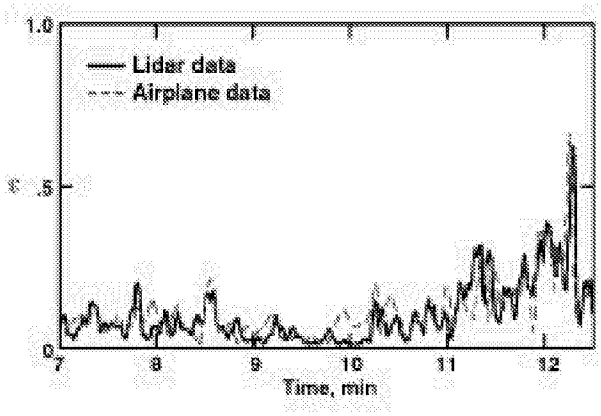

Figure 3.2.2-4 Comparison of lidar-derived and airplane-derived epsilon.

As we can see, the epsilon measured with the lidar correlates quite well with that which is observed at the airplane. The cross-correlation of these two quantities is .95.

4. CONCLUDING REMARKS

A flight test of a coherent lidar system was conducted over the Front Range region of the Rocky Mountains in the general vicinity of Denver, Colorado. Over a period of close to 2 weeks, 15 flight hours were accumulated during 6 flights in a Lockheed Electra L-188 modified as an atmospheric research aircraft and operated by the National Center for Atmospheric Research from the Jefferson County Airport near Broomfield, Colorado. Flight altitudes ranged from 5,000 to 25,000 ft mean sea level (MSL) and encountered light to moderate turbulence under wind shear, convective, and mountain-wave conditions. Backscatter conditions ranged from mostly clear to occasional clouds and virga. Minimal backscatter conditions at altitudes near 25,000 ft were comparable to low springtime aerosol concentrations over the Pacific Ocean (substantially below average). This flight test of a coherent lidar system has demonstrated this approach as a technique for remotely detecting atmospheric turbulence in clear air conditions at ranges of up to 8 km. Both time-to-encounter and the strength of the turbulence correlated well with onboard normal acceleration and sensor data as well as with the turbulence intensity perceptions of the onboard aircraft research staff. No turbulence was encountered that had not been detected by the lidar.

5. REFERENCES

Bowles, Roland, former Project Manager of NASA-FAA Wind Shear Program, private communication, December 1998.

Frehlich, Rod, Stephen M. Hannon and Sammy W. Henderson, "Coherent Doppler Lidar Measurements of Wind Field Statistics," Boundary-Layer Meteorol. 86, pp. 233–256, 1998.

Frehlich, Rod, Stephen M. Hannon and Sammy W. Henderson, "Performance of a 2-μm Coherent Doppler Lidar for Wind Measurements," *J. Atmos. Oceanic Technol.,* vol. 11, no. 6, p. 1517, December 1994.

Huffaker, R. Milton and R. Michael Hardesty, "Remote Sensing of Atmospheric Wind Velocities Using Solid-State and CO_2 Coherent Laser Systems," Proceedings IEEE, vol. 84, no. 2, p. 181 February 1996.

Soreide, David, Rodney K. Bogue, Jonathan Seidel, L. J. Ehernberger, *The Use of a Lidar Forward-Looking Turbulence Sensor for Mixed-Compression Inlet Unstart Avoidance and Gross Weight Reduction on a High Speed Civil Transport*, NASA Technical Memorandum 104332, July 1997.

REPORT DOCUMENTATION PAGE

Form Approved
OMB No. 0704-0188

1. AGENCY USE ONLY (Leave blank)	2. REPORT DATE	3. REPORT TYPE AND DATES COVERED
	September 2000	Meeting Paper

4. TITLE AND SUBTITLE

Airborne Coherent Lidar for Advanced In-Flight Measurements (ACLAIM) Flight Testing of the Lidar Sensor

5. FUNDING NUMBERS

WU 577-40-30-E8-42-00-ACL

6. AUTHOR(S)

David C. Soreide, Rodney K. Bogue,
L. J. Ehernberger, Stephen M. Hannon, and David A. Bowdle

7. PERFORMING ORGANIZATION NAME(S) AND ADDRESS(ES)

NASA Dryden Flight Research Center
P.O. Box 273
Edwards, California 93523-0273

8. PERFORMING ORGANIZATION REPORT NUMBER

H-2428

9. SPONSORING/MONITORING AGENCY NAME(S) AND ADDRESS(ES)

National Aeronautics and Space Administration
Washington, DC 20546-0001

10. SPONSORING/MONITORING AGENCY REPORT NUMBER

H-2428

11. SUPPLEMENTARY NOTES

Prepared for the American Meteorological Society 9th Conf. on Aviation, Range, and Aerospace Meteorology, Orlando, FL, Sept. 11–15, 2000. David Soreide, Boeing Co.; Rodney Bogue and L. J. Ehernberger, NASA Dryden Flight Research Center; Stephen Hannon, Coherent Technologies, Inc.; and David Bowdle, Univ. of Alabama at Huntsville.

12a. DISTRIBUTION/AVAILABILITY STATEMENT

Unclassified—Unlimited
Subject Category 03, 06

This report is available at http://www.dfrc.nasa.gov/DTRS/

12b. DISTRIBUTION CODE

13. ABSTRACT (Maximum 200 words)

The purpose of the ACLAIM program is ultimately to establish the viability of light detection and ranging (lidar) as a forward-looking sensor for turbulence. The goals of this flight test are to: 1) demonstrate that the ACLAIM lidar system operates reliably in a flight test environment, 2) measure the performance of the lidar as a function of the aerosol backscatter coefficient (β), 3) use the lidar system to measure atmospheric turbulence and compare these measurements to onboard gust measurements, and 4) make measurements of the aerosol backscatter coefficient, its probability distribution and spatial distribution. The scope of this paper is to briefly describe the ACLAIM system and present examples of ACLAIM operation in flight, including comparisons with independent measurements of wind gusts, gust-induced normal acceleration, and the derived eddy dissipation rate.

14. SUBJECT TERMS

Atmospheric turbulence, Coherent lidar, Doppler lidar, Flight test, Optical radar, Structure function, Turbulence detection.

15. NUMBER OF PAGES

8

16. PRICE CODE

A02

17. SECURITY CLASSIFICATION OF REPORT	18. SECURITY CLASSIFICATION OF THIS PAGE	19. SECURITY CLASSIFICATION OF ABSTRACT	20. LIMITATION OF ABSTRACT
Unclassified	Unclassified	Unclassified	Unlimited